# Metal coordination induced time-dependent phosphorescence colors (TDPC) in multi-component doped films for multifunctional applications

Zepeng Wang,[a,b,†] Lan Zhang,[c,†] Mengjiao Dong,[a] Yingjie Xie,[b] Peng Yu,[b] Xiaoqin Guo,[b] Fu-shun Liang,*[,a] Jianfeng Zhao,*[,b] and Yun Geng*[,c]

[a] Institute of Organic Luminescent Materials (IOLM), College of Chemistry, Liaoning University, Shenyang 110036, PR China
[b] Key Laboratory of Flexible Electronics (KLOFE), Institute of Advanced Materials (IAM), School of Flexible Electronics (SoFE), Jiangsu National Synergetic Innovation Center for Advanced Materials (SICAM), Nanjing Tech University (Nanjing Tech), Nanjing 211816, PR China
[c] Institute of Functional Material Chemistry, Faculty of chemistry, Northeast Normal University, 5268 Renmin Street, Changchun, 130024, Jilin, PR China

## Contents

### 1. Materials

(4-([2,2':6',2''-terpyridin]-4'-yl)phenyl)boronic acid (TPy-BA) was purchased from Shanghai Bidepharm. The zinc chloride ($ZnCl_2$), zinc perchlorate ($Zn(ClO_4)_2$), sodium iodide (NaI) were purchased from Macklin. The zinc iodide ($ZnI_2$) was purchased from Bidepharm. The zinc bromide ($ZnBr_2$) was purchased from 3Achem. The zinc acetate ($Zn(OAc)_2$) was purchased from Meryer. The zinc trifluorosulfonate ($Zn(CF_3SO_3)_2$) was purchased from Leyan. Polyvinyl alcohol (PVA-1799) with the alcoholysis degree of 98-99% was purchased from General-reagent. All the chemicals were used directly without further purification.

### 2. Experimental section

#### 2.1 Preparation of Polymer Matrices

PVA (1 g) was dissolved in deionized water ($H_2O$) (34 mL) at 95 °C for 2 h. The obtained PVA aqueous solutions (30 mg/mL) after the filtration were used for the following experiments.

#### 2.2 Preparation of Transparent Films

PVA (1 g) was dissolved in deionized water ($H_2O$) (34 mL) at 95 °C for 2 h. The obtained PVA aqueous solutions (30 mg/mL) after the filtration were used for the following experiments. TPy-BA (0.01, 0.05, 0.1, 0.3, 0.5, and 1 mg/mL) ethanol solutions were dispersed in the PVA aqueous solutions. The homogeneous solutions were prepared after the ultrasonication for 5 h followed by standing for 1 h. Then, the films were produced with the drop-casting approach using these solutions on 20 mm × 20 mm quartz plate. After drying at 60 °C for 3 h, transparent films were obtained. For salts doped films, these different salts aqueous solutions were added into the mixed solution containing PVA and TPy-BA before ultrasonication. For doping two salts aqueous solutions, the prepared two salts aqueous solutions were added into the mixed solution containing PVA and TPy-BA before ultrasonication.

### 3. Measurements and methods

#### 3.1 Instruments

The UV-vis absorption spectra were determined on a Shimadzu UV-1780 spectrophotometer. The photoluminescence spectra and phosphorescence emission spectra were performed at room temperature on a Hitachi F-7100 spectrometer. The lifetimes of fluorescence and phosphorescence spectra were measured on Edinburgh FLS980 using a time-correlated single-photon (TCSPC) module spectrometer. The absolute photoluminescence quantum yields (PLQY) were obtained on the Edinburgh FLS980 spectrometer with an integrating sphere. The Nuclear Magnetic Resonance Hydrogen Spectra (^{1}H NMR) were obtained on JNM-ECZ400S/L1. Powder X-ray diffraction (XRD) measurements were measured on Smartlab (3 KW) using Cu $K\alpha$

radiation with $2\vartheta$ range of 5-40°, 40 KeV, and 30 mA having a scanning rate of 0.01° s$^{-1}$ ($2\vartheta$) at room temperature.

**3.2 Phosphorescence quantum yields**

The phosphorescence quantum yields of all the doped PVA films were obtained following the equation

$$\Phi_{phos} = \frac{B}{A} \times \Phi_{PL}$$

where A and B represent the integral areas of total photoluminescence and phosphorescence spectra, respectively.

**3.3 Computational details**

All the geometry structures, electronic structures and relevant photophysical properties were explored in the Gaussian 16[1] and ADF 2016[2] program packages. We employed 6-311G** basis set for all the atoms except for I atom with Lanl2dz basis set and B3LYP functional to optimize the molecular structures in gas state. The differences of the geometric structures between the ground and excited states were calculated and characterized with root-mean-square deviations (RMSD) which are plotted in the VMD program.[3] The ADF 2016 program package was employed to calculate the spin-orbital coupling (SOC) matrix elements between the singlet and triplet states with the B3LYP functional and the ZORA/DZP basis set.[4] And the natural transition orbitals (NTOs) were analyzed and plotted in Multiwfn 3.8 package.[5] In addition, the reorganization energy and Huang-Ryhs factor were calculated using MOMAP software.[6-7] The corresponding calculation results were obtained through optimized molecular structures in gas state without consideration about weak interaction.

Moreover, the exciton binding energy can be calculated according to the following formula:

$$E_k^a - E = \varepsilon_a - \varepsilon_k - [(kk|aa) - (ka|ak)]$$

In the above equation, $E_k^a - E$ is the excitation energy, $\varepsilon_a - \varepsilon_k$ is the energy gap between HOMO and LUMO, $[(kk|aa) - (ka|ak)]$ is the exciton binding energy where $(kk|aa)$ is the coulomb points and $(ka|ak)$ is the switch points.
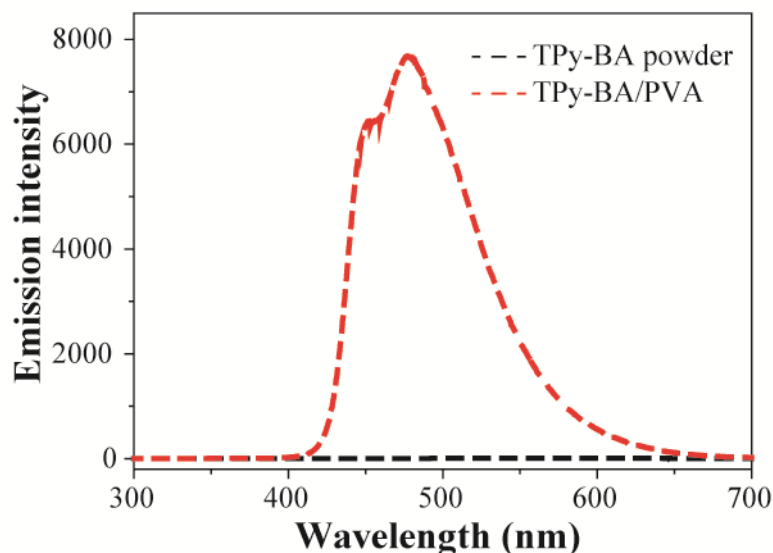
**4. Supplementary figures and tables**



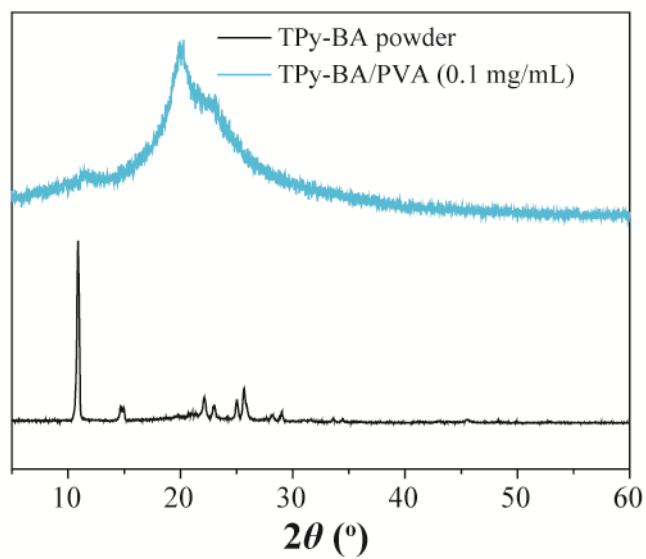**Figure S1** The phosphorescence intensity contrast of TPy-BA powder and TPy-BA/PVA film.

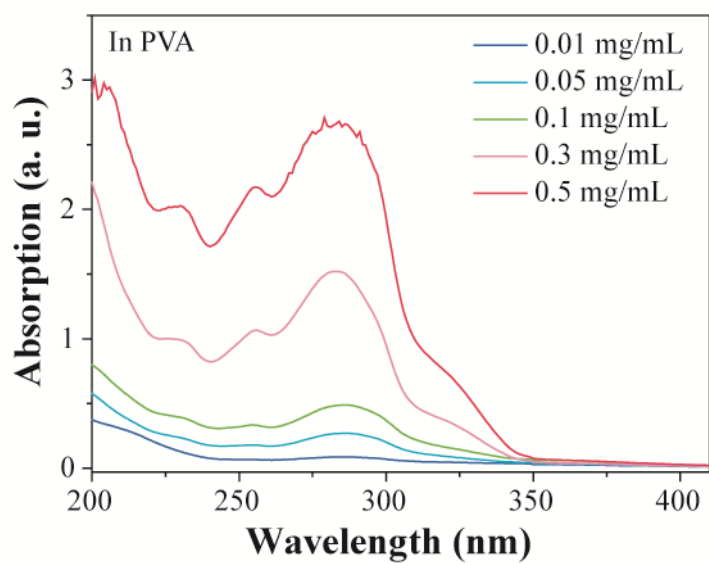**Figure S2** The XRD spectra of TPy-BA powder and TPy-BA/PVA film.



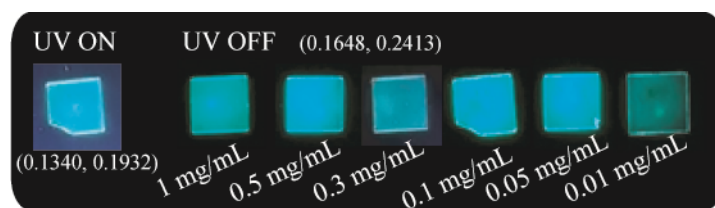**Figure S3** The absorption spectra of TPy-BA/PVA film.



**Figure S4** The photographs of TPy-BA/PVA films with different concentrations.
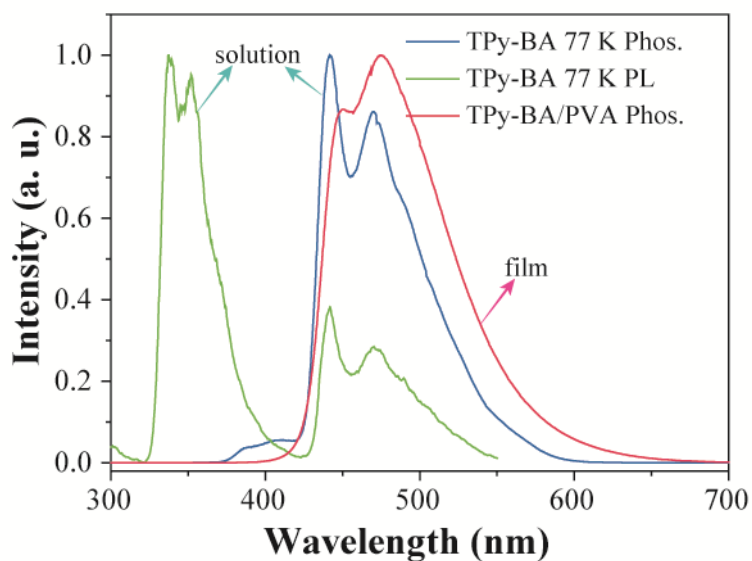
**Figure S5** The comparison of TPy-BA/PVA phosphorescent spectrum film in ambient condition, TPy-BA ethanol solution in 77 K and PL spectrum of TPy-BA in 77 K.

**Table S1** The phosphorescent lifetime and efficiency of TPy-BA/PVA with different concentrations.

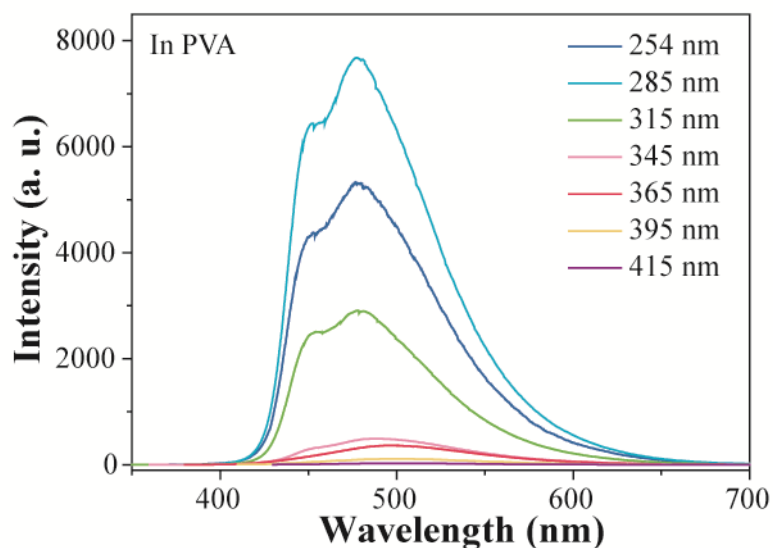|                   | 0.01 mg/mL | 0.05 mg/mL | 0.1 mg/mL | 0.3 mg/mL | 0.5 mg/mL | 1 mg/mL |
| ----------------- | ---------- | ---------- | --------- | --------- | --------- | ------- |
| Lifetime (ms)     | 111.28     | 86.78      | 99.13     | 100.51    | 130.73    | 143.25  |
| Phos. efficiency  | 5.35%      | 5.41%      | 3.90%     | 4.73%     | 4.45%     | 3.49%   |



**Figure S6** The excitation-dependent phosphorescence spectra of TPy-BA/PVA film (0.1 mg/mL).
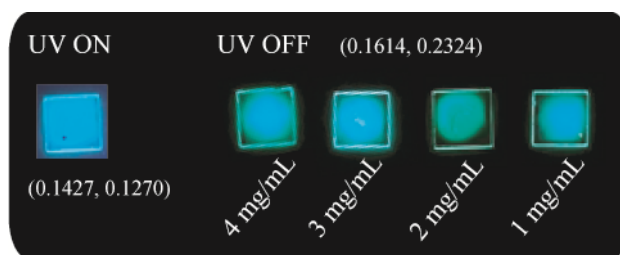
**Figure S7** The photographs of TPy-BA/ZnCl$_2$/PVA with different doping concentrations of ZnCl$_2$ solutions.
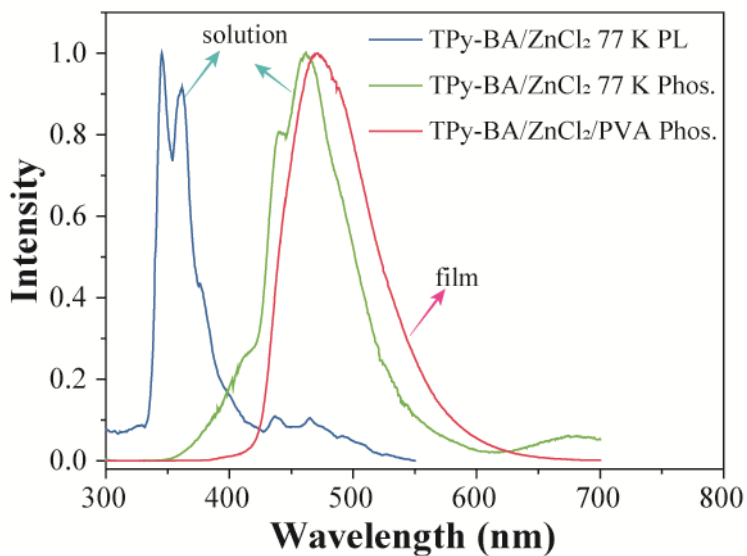


**Figure S8** The comparison of TPy-BA/ZnCl$_2$/PVA phosphorescent spectrum in ambient condition, TPy-BA@ZnCl$_2$ ethanol solution in 77 K and PL spectrum of TPy-BA@ZnCl$_2$ in 77 K.

**Table S2** The phosphorescent lifetime and efficiency of TPy-BA/ZnCl$_2$/PVA with different ZnCl$_2$ solution concentrations.

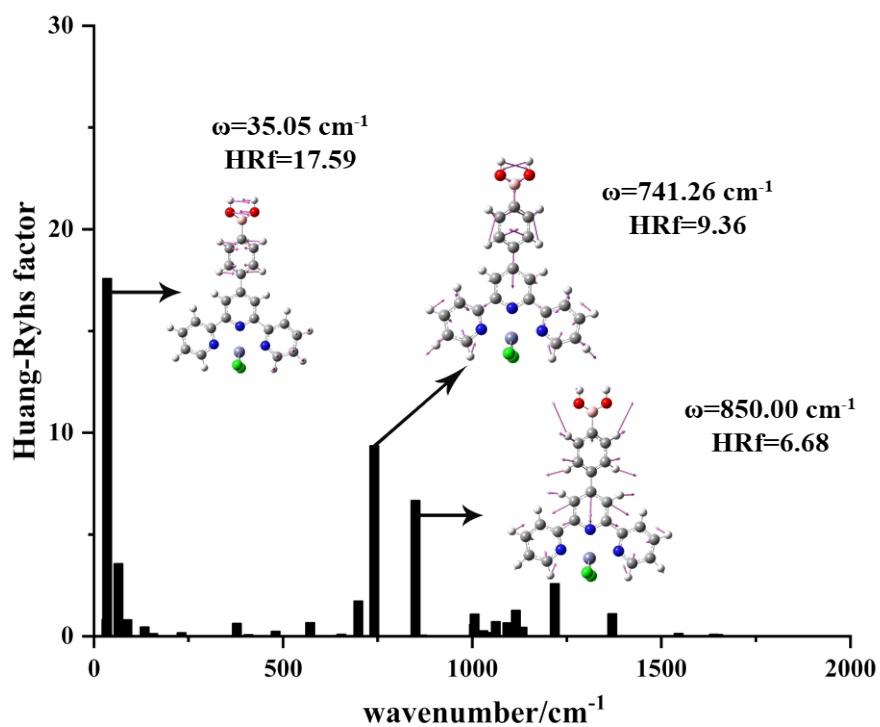|                  | 1 mg/mL | 2 mg/mL | 3 mg/mL | 4 mg/mL |
|------------------|---------|---------|---------|---------|
| Lifetime (ms)    | 129.37  | 187.97  | 218.75  | 310.87  |
| Phos. efficiency | 6.65%   | 7.47%   | 6.51%   | 7.07%   |

**Figure S9** The total HRf factor of TPy-BA/ZnCl$_2$ in T$_1$ state.
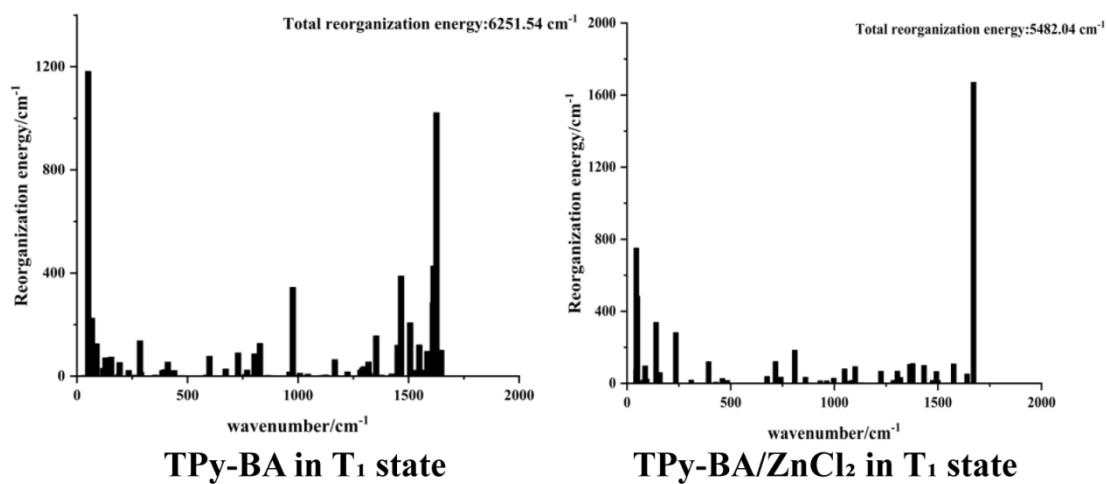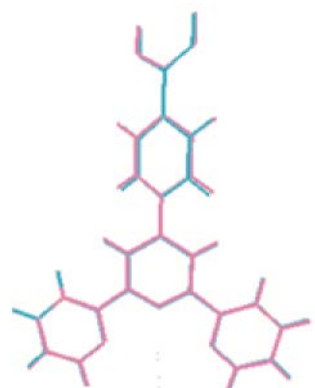


**Figure S10** The total reorganization energy of TPy-BA and TPy-BA/ZnCl$_2$ in T$_1$ state.

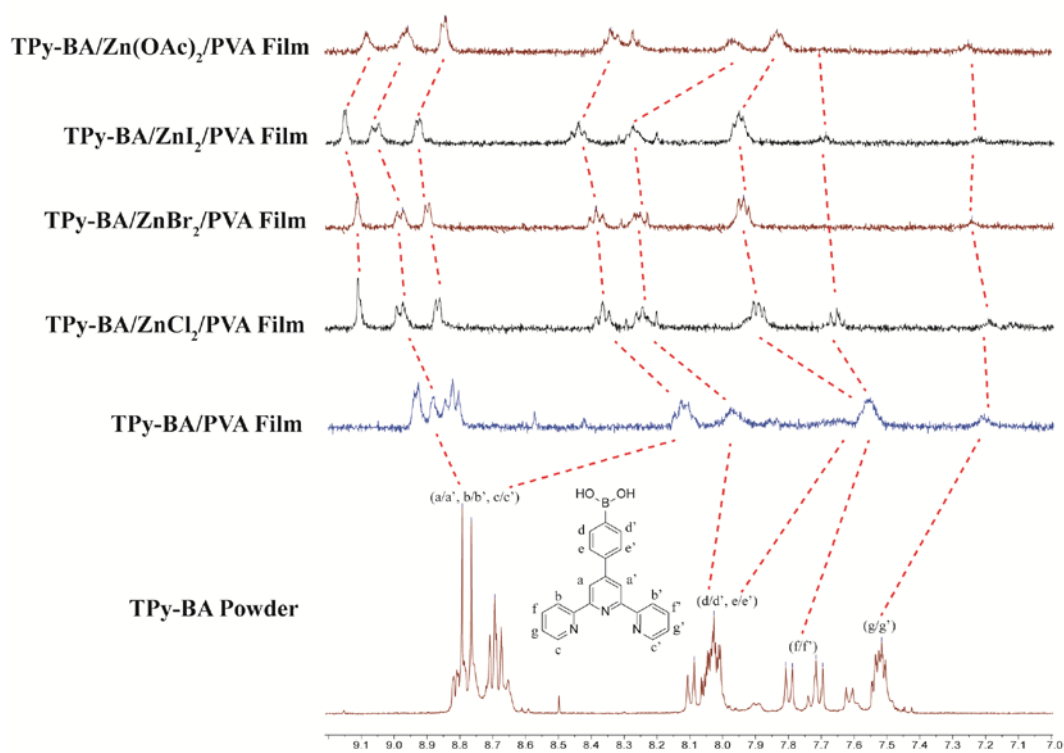RMSD value: 0.30 Å

**Figure S11** The RMSD value of TPy-BA/ZnI$_2$ in T$_1$ state.



**Figure S12** The $^1$H NMR spectra of TPy-BA powder and TPy-BA/PVA, TPy-BA/ZnCl$_2$/PVA, TPy-BA/ZnBr$_2$/PVA, TPy-BA/ZnI$_2$/PVA, TPy-BA/(OAc)$_2$/PVA.
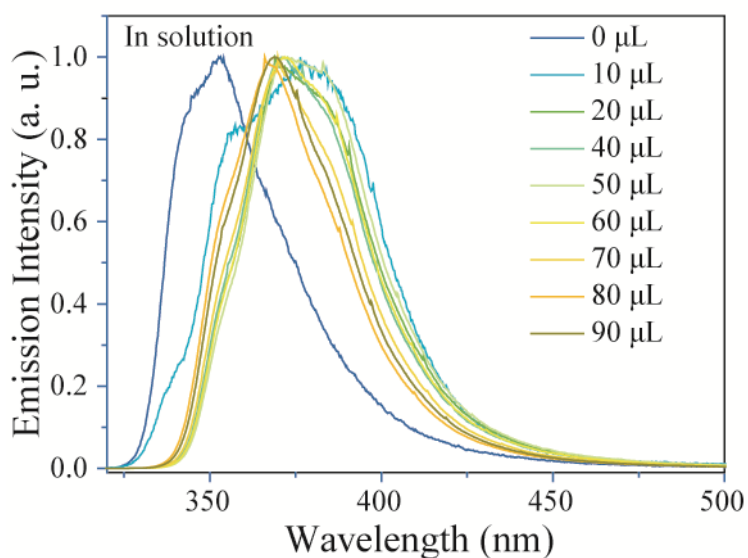
**Figure S13** The fluorescence emission spectra of TPy-BA ethanol solution with doping different amount $ZnCl_2$ aqueous solution.
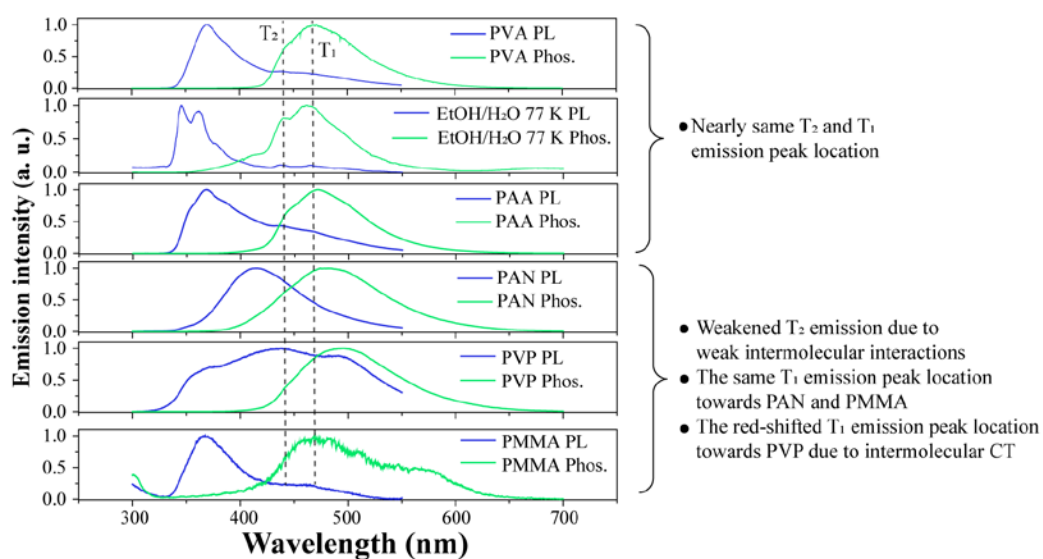


**Figure S14** The PL and phosphorescence spectra of TPy-BA/$ZnCl_2$ in low-temperature (77 K) and different matrixes.

**Table S3** The SOC value between excited Sn and Tn of TPy-BA, TPy-BA/$ZnCl_2$ and TPy-BA/$ZnI_2$.

| | TPy-BA | | TPy-BA/$ZnCl_2$ | | TPy-BA/$ZnI_2$ | |
|---|---|---|---|---|---|---|
| n | $S_n$ | $T_n$ | $S_n$ | $T_n$ | $S_n$ | $T_n$ |
| 1 | 4.20 | 3.14 | 3.41 | 2.94 | 2.53 | 2.52 |

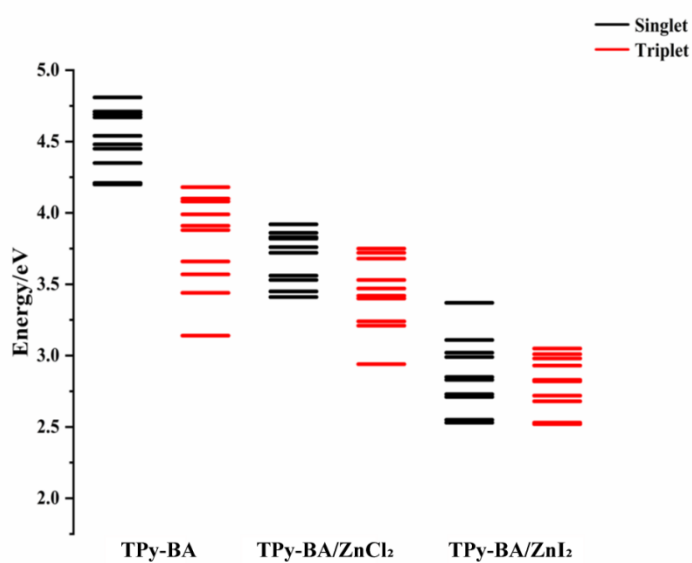| | | | | | | |
|---|---|---|---|---|---|---|
| 2 | 4.21 | 3.44 | 3.45 | 3.21 | 2.55 | 2.53 |
| 3 | 4.35 | 3.57 | 3.53 | 3.24 | 2.71 | 2.68 |
| 4 | 4.45 | 3.66 | 3.56 | 3.40 | 2.73 | 2.72 |
| 5 | 4.48 | 3.88 | 3.72 | 3.42 | 2.83 | 2.82 |
| 6 | 4.54 | 3.91 | 3.76 | 3.47 | 2.85 | 2.83 |
| 7 | 4.67 | 3.99 | 3.82 | 3.53 | 2.99 | 2.93 |
| 8 | 4.69 | 4.08 | 3.83 | 3.68 | 3.02 | 2.98 |
| 9 | 4.71 | 4.10 | 3.86 | 3.72 | 3.11 | 3.01 |
| 10 | 4.81 | 4.18 | 3.92 | 3.75 | 3.37 | 3.05 |



**Figure S15** The energy level of TPy-BA, TPy-BA/ZnCl$_2$ and TPy-BA/ZnI$_2$.

**Table S4** The spin-orbit coupling constants between S$_1$ and different triplet energy level.

| | TPy-BA | TPy-BA/ZnCl$_2$ | TPy-BA/ZnI$_2$ |
|---|---|---|---|
| | | | |

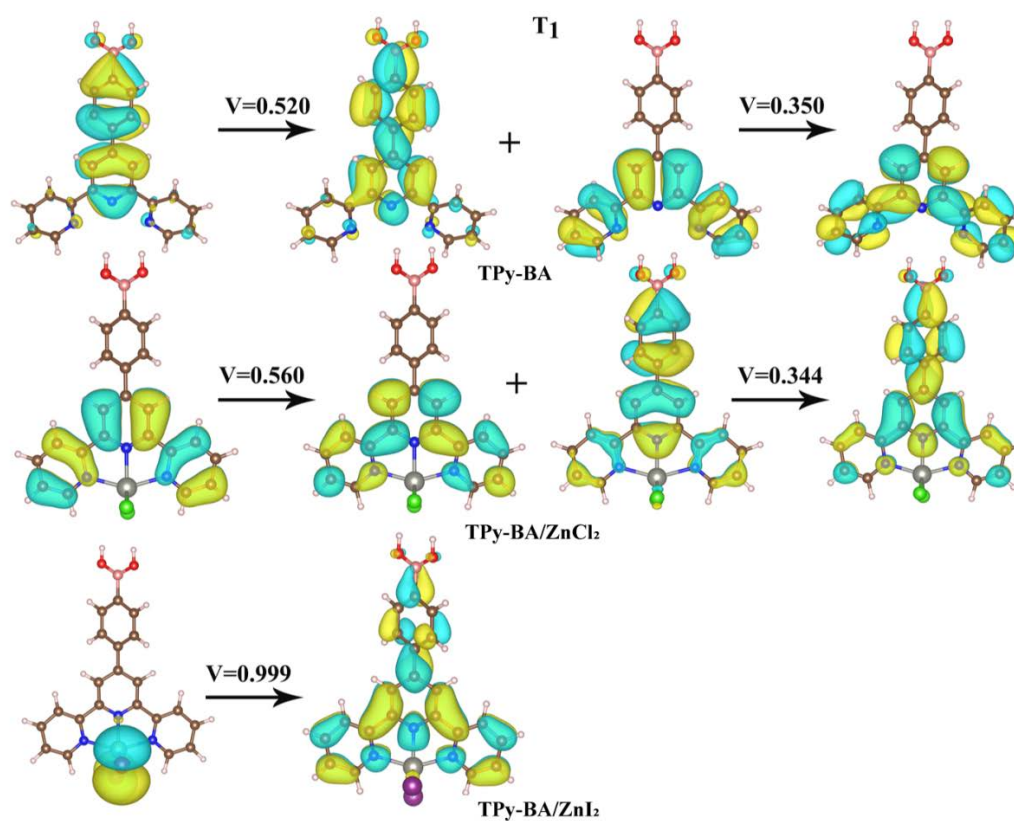| | | | |
|---|---|---|---|
| T$_1$ | 5.06 | 5.76 | 6.83 |
| T$_2$ | 0.937 | 137 | 114 |
| T$_3$ | 0.166 | 83.1 | 66.2 |
| T$_4$ | 0.761 | 95.3 | 30.3 |
| T$_5$ | 1.69 | 9.19 | 66.3 |
| T$_6$ | 0.651 | 0.727 | 5.78 |
| T$_7$ | 0.955 | 7.76 | 32.7 |
| T$_8$ | 0.34 | 3.18 | 3.89 |
| T$_9$ | 2.13 | 27.9 | 41.5 |
| T$_{10}$ | 6.00 | 32.1 | 10.7 |



**Figure S16** The natural transition orbit (NTO) of TPy-BA, TPy-BA/ZnCl$_2$ and TPy-BA/ZnI$_2$ in T$_1$ state.
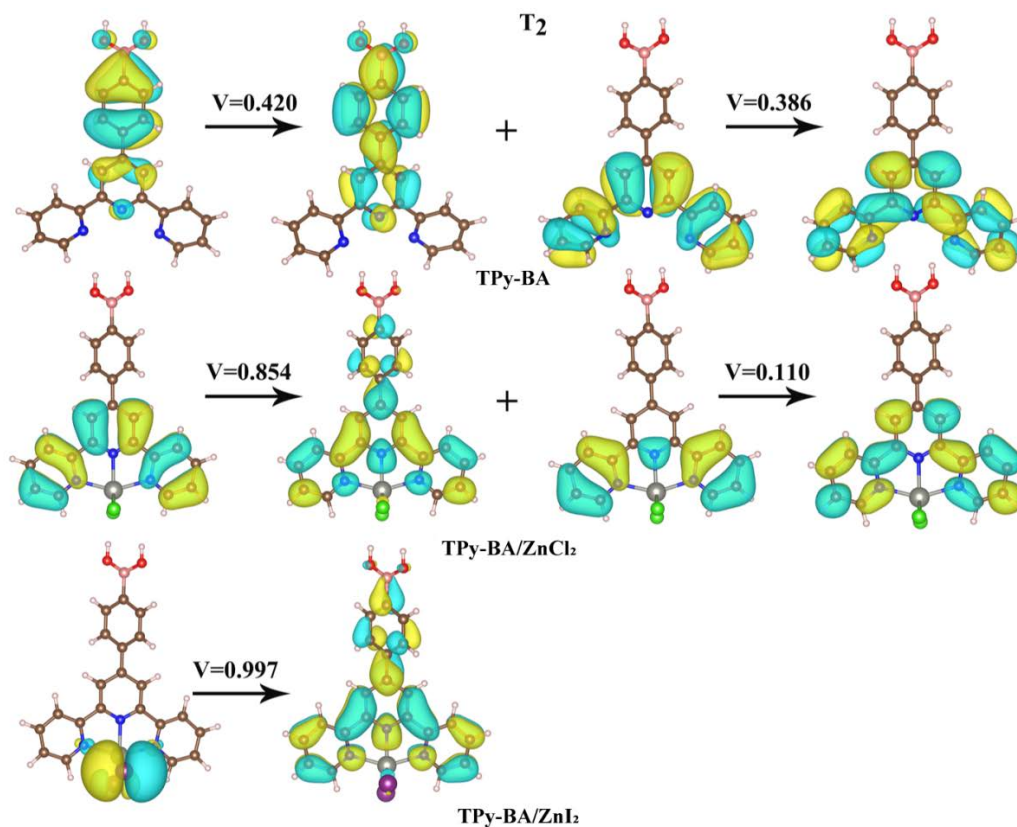
**Figure S17** The natural transition orbit (NTO) of TPy-BA, TPy-BA/$ZnCl_2$ and TPy-BA/$ZnI_2$ in $T_2$ state.

**References:**

1. M. J. Frisch, G. W. Trucks, H. B. Schlegel, G. E. Scuseria, M. A. Robb, J. R. Cheeseman, G. Scalmani, V. Barone, G. A. Petersson, H. Nakatsuji, X. Li, M. Caricato, A. V. Marenich, J. Bloino, B. G. Janesko, R. Gomperts, B. Mennucci, H. P. Hratchian, J. V. Ortiz, A. F. Izmaylov, J. L. Sonnenberg, D. W. Young, F. Ding, F. Lipparini, F. Egidi, J. Goings, B. Peng, A. Petrone, T. Henderson, D. Ranasinghe, V. G. Zakrzewski, J. Gao, N. Rega, G. Zheng, W. Liang, M. Hada, M. Ehara, K. Toyota, R. Fukuda, J. Hasegawa, M. Ishida, T. Nakajima, Y. Honda, O. Kitao, H. Nakai, T. Vreven, K. Throssell, J. J. Montgomery, J. E. Peralta, F. Ogliaro, M. J. Bearpark, J. J. Heyd, E. N. Brothers, K. N. Kudin, V. N. Staroverov, T. A. Keith, R. Kobayashi, J. Normand, K. Raghavachari, A. P. Rendell, J. C. Burant, S. S. Iyengar, J. Tomasi, M. Cossi, J. M. Millam, M. Klene, C. Adamo, R. Cammi, J. W. Ochterski, R. L. Martin, K. Morokuma, O. Farkas, J. B. Foresman and D. J. Fox, Gaussian 16, Revision C.01, Wallingford CT: Gaussian Inc, 2019.
2. ADF, SCM, Theoretical Chemistry, Virje Universiteit, Amsterdam, The Netherlands, 2016.
3. W. Humphrey, A. Dalke and K. Schulten, *J. Mol. Graph.*, 1996, **14**, 33-38.
4. E. van Lenthe, J. G. Snijders and E. J. Baerends, *J. Chem. Phys.*, 1996, **105**, 6505-6516.
5. T. Lu and F.W. Chen, *J. Comput. Chem.*, 2012, **33**, 580-592.
6. Y.L. Niu, Q. Peng, C.M. Deng, X. Gao and Z.G. Shuai, *J. Phys. Chem. A.*, 2010**, 114,** 7817-7831.
7. Q. Peng, Y.P. Yi and Z.G. Shuai, *J. Am. Chem. Soc.*, 2007, **129,** 9333-9339.